J Incl Phenom Macrocycl Chem (2015) 82:497–504
DOI 10.1007/s10847-015-0531-x

ORIGINAL ARTICLE

Cyclodextrin inclusion compound crystals for growth of Cu–Au core–shell nanoparticles

Nataly Silva[1] · Esteban Arellano[1] · Carmen Castro[1] · Nicolás Yutronic[1] · Erika Lang[2] · Boris Chornik[3] · Paul Jara[1]

Received: 9 December 2014 / Accepted: 5 May 2015 / Published online: 9 May 2015

Abstract The preparation and structural elucidation of the 2α-cyclodextrin/decylamine inclusion compound (IC) by proton nuclear magnetic resonance, rotating frame overhauser effect spectroscopy and powder X-ray diffraction have been achieved. The IC microcrystals were used as a support for the preparation of Au–Cu core–shell nanoparticles by the sputtering method. The coating of copper nanoparticles with gold was verified through anodic stripping voltammetry. The presence of metallic copper and the absence of copper oxides were determined by X-ray photoelectron spectroscopy. These results show that the formation of core–shell Cu–Au by sputtering is an effective approach to prevent the oxidation of Cu particles, leading to potential applications in nanoelectronics.

Graphical Abstract

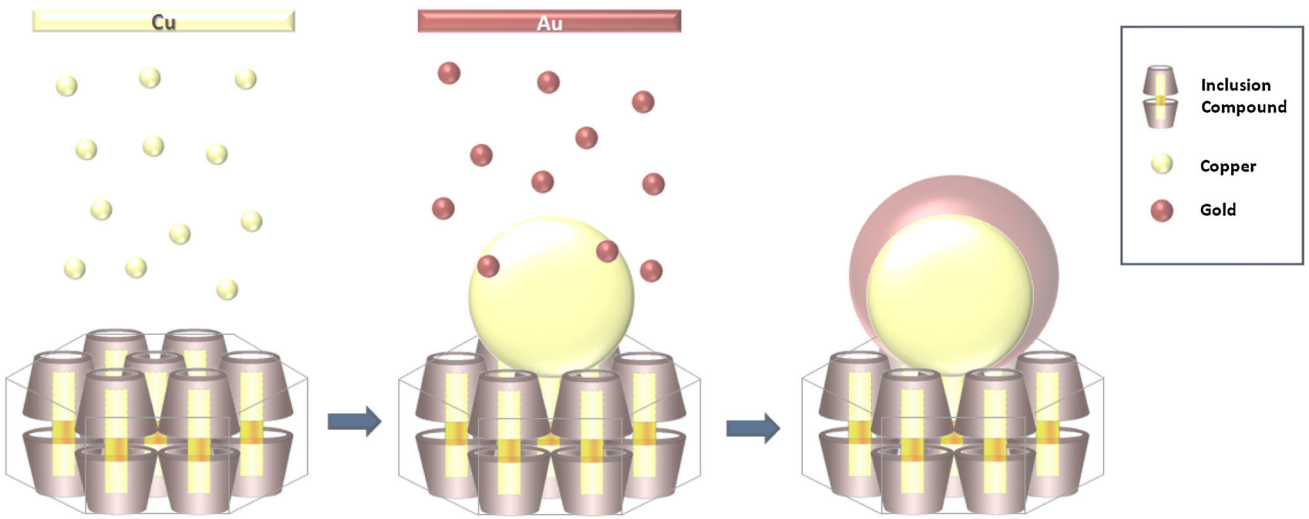

Keywords α-Cyclodextrin · Decylamine · Inclusion compound · Copper nanoparticles · Gold nanoparticles · Core–shell nanoparticles

✉ Paul Jara
pjara@uchile.cl

[1] Department of Chemistry, Universidad de Chile, Las Palmeras, 3425 Santiago, Chile

[2] Department of Biology, CEM, Universidad de Chile, Las Palmeras, 3425 Santiago, Chile

[3] Department of Physics, Universidad de Chile, Beauchef, 850 Santiago, Chile

Introduction

Cyclodextrin (CD) inclusion compounds (IC) are widely used in pharmaceutical science, separation technology, and more recently in the nanoscience field. In this last example,

CD has been used for the phase transfer of nanoparticles (NPs) in liquids of different polarities [1, 2] and to prepare colloidal gold nanoparticles (AuNPs) by chemical reduction in the presence of unmodified CD [3], thiolated α- and β-CDs [4] and by femtosecond laser ablation [5].

In some cases, CD ICs can be crystallized in single crystals, such as supramolecular assemblies constructed by noncovalent bonds between two CD cones. These anisotropic crystals possess faces with different chemical properties because of the symmetry of the unit cell of CD and the shape of the organic molecules included as well as their anisotropic arrangements in the crystals [6].

Recently, CD ICs have been used for the preparation of NPs. The most recent method utilizes the surface functionality of a specific plane of IC crystals, where the surface functional groups (–SH, $–NH_2$ or –COOH) are provided by the guest molecules. This concept involved supramolecular chemistry and nanochemistry [7, 8].

In α-CD-alkyl guest IC crystals, the functional groups of the guest molecules are located at the CD cone extremity in the electron-rich areas, whereas the hydrocarbon chains are located in the relatively apolar cavities [9]. The functional groups (–SH [10, 11], –COOH [12], or $–NH_2$ [13, 14]) located in the opening of the CD are available to interact with the stabilizing particles.

In this regard, copper nanoparticles (CuNPs) have been obtained through various methods, such as chemical reduction [15], thermal reduction [16], vacuum vapour deposition [17], and microwave irradiation [18], among others [19, 20]. CuNPs have antifungal and bacteriostatic properties that offer potential applications in nanomedicine, water treatment and food industries [21–25]. Moreover, an application of great interest is the use of CuNPs in nanoelectronic components, leveraging their conductive properties [26].

However, the use of CuNPs is limited because of rapid surface oxidation, forming mostly cuprous oxide (Cu_2O) and a smaller amount of cupric oxide (CuO) [27]. Various protection methods have been reported to prevent the oxidation of CuNPs, such as encapsulation in a matrix [28, 29] or creating colloidal copper nanoshells [30].

In this work, the preparation of Au–Cu core–shell nanoparticles (Au–CuNPs) by the sputtering method is proposed, using α-cyclodextrin (α-CD) with decylamine (DA) guest molecules as a microcrystal support (Scheme 1).

Results and discussion

Proton nuclear magnetic resonance (^{1}H-NMR) was used to confirm the formation of IC and determine the host–guest intermolecular interactions. Tables 1 and 2 show the chemical shifts of DA and α-CD molecules. An upfield shift of the guest molecule protons as a result of the total inclusion

Table 1 ^{1}H-NMR chemical shifts, δ (ppm), and Δδ, of pure DA (DMSO-d_6 solvent) and that included in the α-cyclodextrin matrix

Guest	$–CH_3$ (ppm)	$–(CH_2)n–$ (ppm)	$–CH_2–$ (ppm)
DA	0.89	1.27	1.51
α-CD/DA	0.82	1.20	1.30
Δδ[a]	0.07	0.07	0.21
Integration	3		

[a] $\Delta\delta = \delta_{\text{pure DA}} - \delta_{\text{DA complex}}$

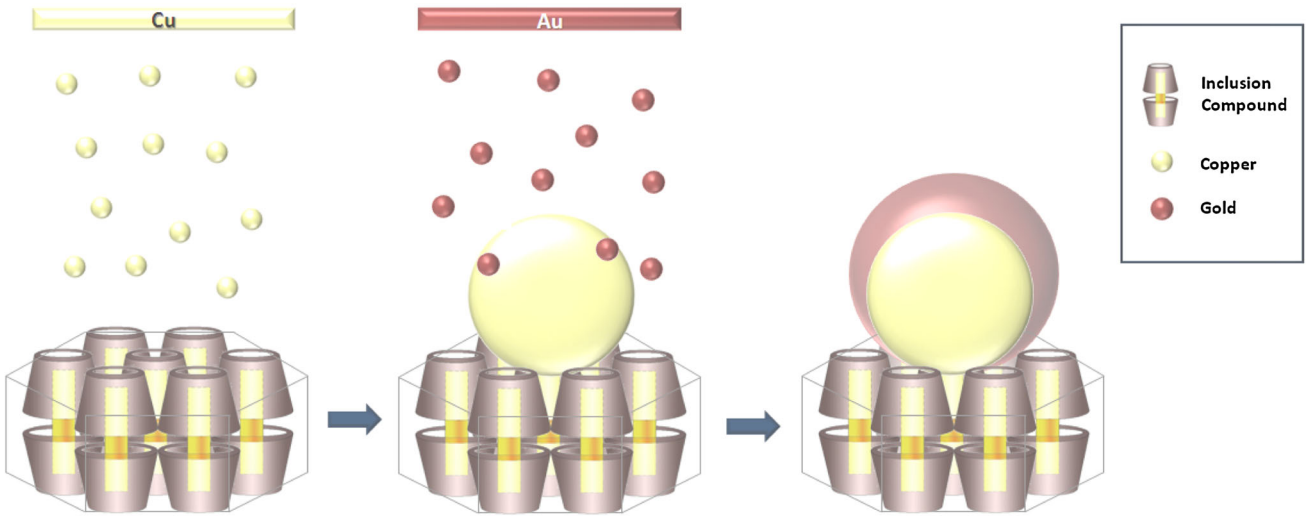

Scheme 1 Representation of the deposition of copper and gold on the (001) plane of the IC crystal, where the $–NH_2$ groups of the guest molecule interact with the formed Au–CuNPs

Table 2 ^{1}H-NMR chemical shifts, δ (ppm), and Δδ of native α-CD and α-CD/DA inclusion compound in DMSO-d_6 solvent

Matrix	H1 (ppm)	H2 (ppm)	H3 (ppm)	H4 (ppm)	H5 (ppm)	–OH(2) (ppm)	–OH(3) (ppm)	–OH(6) (ppm)
α-CD	4.80	3.28	3.77	3.37	3.58	5.50	5.43	4.48
α-CD/DA	4.76	3.35	3.73	3.56	3.57	5.40	5.41	4.43
Δδ[a]	0.004	−0.07	0.04	−0.19	0.01	0.10	0.02	0.05
Integration	11.87							

[a] $\Delta\delta = \delta_{\text{native }\alpha-\text{CD}} - \delta_{\text{complex}}$

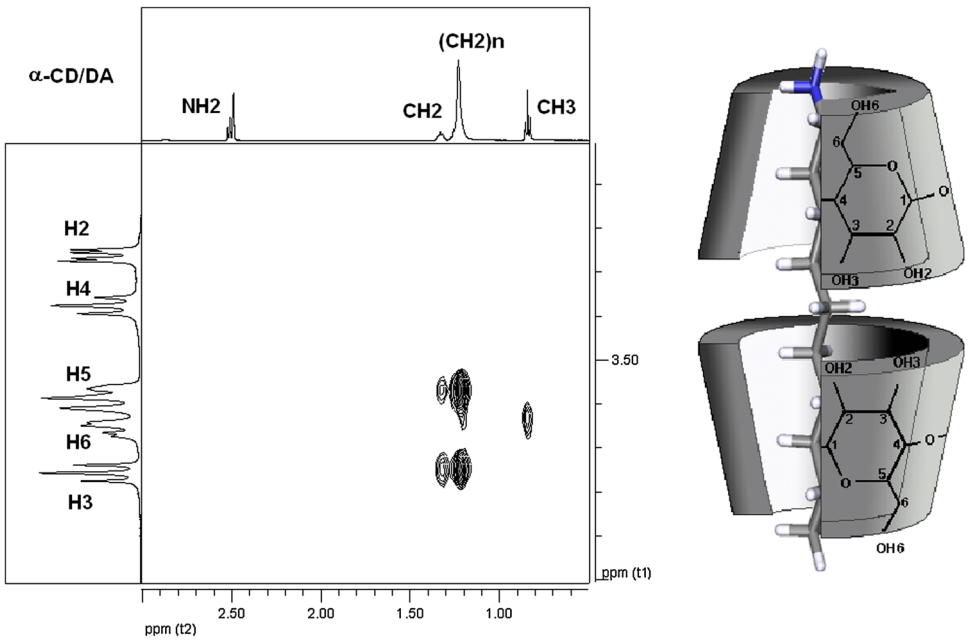

Fig. 1 2D-ROESY spectrum in DMSO-d_6 solvent and schematic representation of α-CD/DA IC. The NH_2 group of the DA guest molecule is represented in *blue*. Cyclodextrin protons are numbered from 1 to 5. (Color figure online)

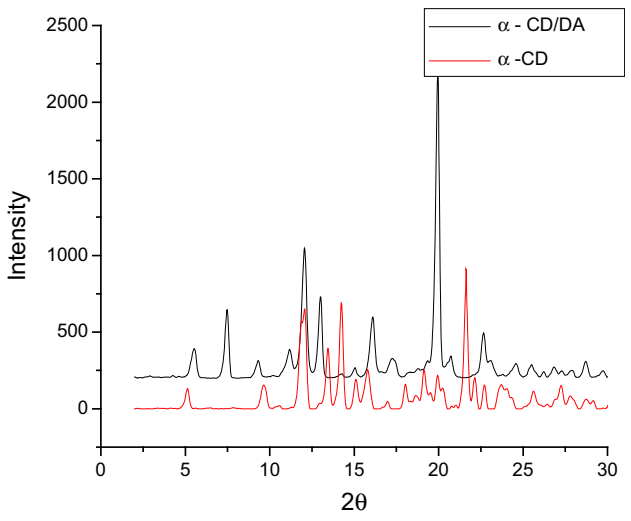

Fig. 2 Powder X-ray diffractogram of native α-CD and α-CD/DA inclusion compounds

within the cavity of the CD was observed. The H-3 and H-5 protons, which are located inside the matrix cavity, experience significant upfield changes in the ^{1}H-NMR chemical shift signals. These results unequivocally confirm the inclusion process.

Using ^{1}H-NMR, the IC stoichiometry was determined by considering the methyl group integration of the guest molecule, which appears at 0.82 ppm upon complexation, as a reference (with an integral of 3) [31]. Subsequently, the integration of the methyl group is compared with a signal of the matrix, e.g. H-1 proton that appears to downfield (4.76 ppm) upon complexation, with an integral of approximately 12. Knowing that each α-CD matrix contains six glucopyranose molecules, it is possible to estimate a host–guest ratio of 2:1 for the IC.

Interactions between the guest molecule DA and the matrix α-CD were identified by rotating frame overhauser effect spectroscopy (2D-ROESY) to determine the IC geometry.

Figure 1 shows the 2D-ROESY spectrum of the IC. Interactions of the CH_2 groups of the alkyl chain corresponding to the guest molecule with the H-3 and H-5 protons, which are found in the cavity of α-CD, were observed, thus confirming the inclusion process. The interaction between the terminal methyl group of the alkyl chain of the guest and the H-6 proton, located at the edge of the smaller opening of α-CD, was also observed.

With the results achieved herein, a head-to-head geometry system is proposed for the α-CD buckets, as shown in Fig. 1.

Phase identification of the IC was performed using powder X-ray diffraction (PXRD) Fig. 2 shows the PXRD patterns of pure α-CD and α-CD/DA IC. All diffractogram planes of IC can be indexed in a crystalline system based on a theoretical hexagonal network. The lattice parameters are: $a = b = 23.7$ Å, $c = 15.9$ Å, $\alpha = \beta = 90^\circ$, and $\gamma = 120^\circ$ [32], (Table 3). The native α-CD crystallizes in an orthogonal system, differing from the α-CD complex. The C-axis values of IC are coincident with the dimensions of a dimer of α-CD, corroborating the stoichiometry of two buckets of CD per each DA guest molecule.

The formation, composition and size of metallic NPs were verified using UV–vis spectrophotometry, transmission electron microscopy (TEM) and scanning electron microscopy–energy dispersive spectrometer (SEM–EDS).

Spectrophotometry is an effective tool for studying the metal type and size of the particles formed by evaluating the peak and shape of the absorption band corresponding to the surface plasmon resonance of nanoparticles.

Figure 3 shows the absorption spectrum of a sample prepared with α-CD/DA microcrystals, which were exposed to sputtering for 15 s with a Cu target and 15 s (3×5 s) with a Au target. An extremely broad absorption band at 548 nm corresponding to resonance of localized surface plasmons of AuNP is observed [33]. A shoulder was also observed in 568 nm. Spectrum of AuNP deposited onto the IC crystals, under the same experimental conditions, shows a single absorption band at 548 nm. This experiment allows us to affirm that the shoulder observed at 568 nm corresponds exclusively to an absorption band of metallic CuNPs [34]. This resonance of localized surface plasmons pattern can be obtained with single and isolated CuNP and AuNP or for the formation of the core–shell Au–CuNP. Spectra obtained from samples of pure native α-CD exposed to sputtering do not exhibit these absorption bands [35].

Figure 4a shows a TEM micrograph of CuNPs obtained by sputtering. Spherical particles with low contrast characteristic of CuNPs are observed. The histogram of a population of 30 particles was obtained. A size dispersity with diameters ranging between 45 and 75 nm was observed.

Figure 4b shows TEM micrographs of CuNPs covered with gold. Spherical particles with great contrast as a result of increased electronic density are observed, which is characteristic of AuNPs. The histogram for a population of 40 particles was obtained. A size dispersity with diameters ranging between 36 and 127 nm was observed.

Mapping using SEM–EDS was performed to identify Au from Cu particles. Figure 5 shows the SEM micrograph and EDS analysis of large particles of about 500 nm embedded in the organic substrate. Composed mainly of carbon (39.1 wt%) and oxygen (58.7 wt%) corresponds to the organic phase of the IC. The particles have a ratio of copper atoms:gold atoms of 15:11.

Additionally, electrochemical studies were performed. The Fig. 6 shows the voltammograms of the IC and the IC conjugated to NPs. The absence of an electrochemical signal was observed for the pure IC voltammogram. For the sample of CuNPs conjugated to IC, an oxidation potential of Cu at +0.17 V appeared [36]. For Au–CuNPs conjugated to IC, the voltammogram signal of the Cu oxidation

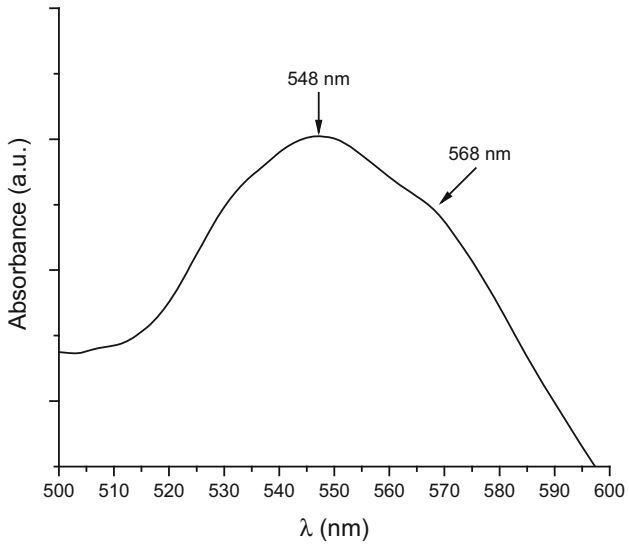

Fig. 3 Absorption spectra of Au–CuNPs on α-CD/DA with 15 s of sputtering for each metal

Table 3 Lattice parameters for α-CD and α-CD IC

Sample	Crystal system	Space group	A (Å)	b (Å)	c (Å)	α (°)	B (°)	γ (°)	Volume Å^3
α-CD	Orthogonal	$P2_12_12_1$	14.89	34.00	6.531	90	90	90	4826.2
α-CD/DA	Hexagonal	P6	23.55	23.55	15.89	90	90	120	7556.6

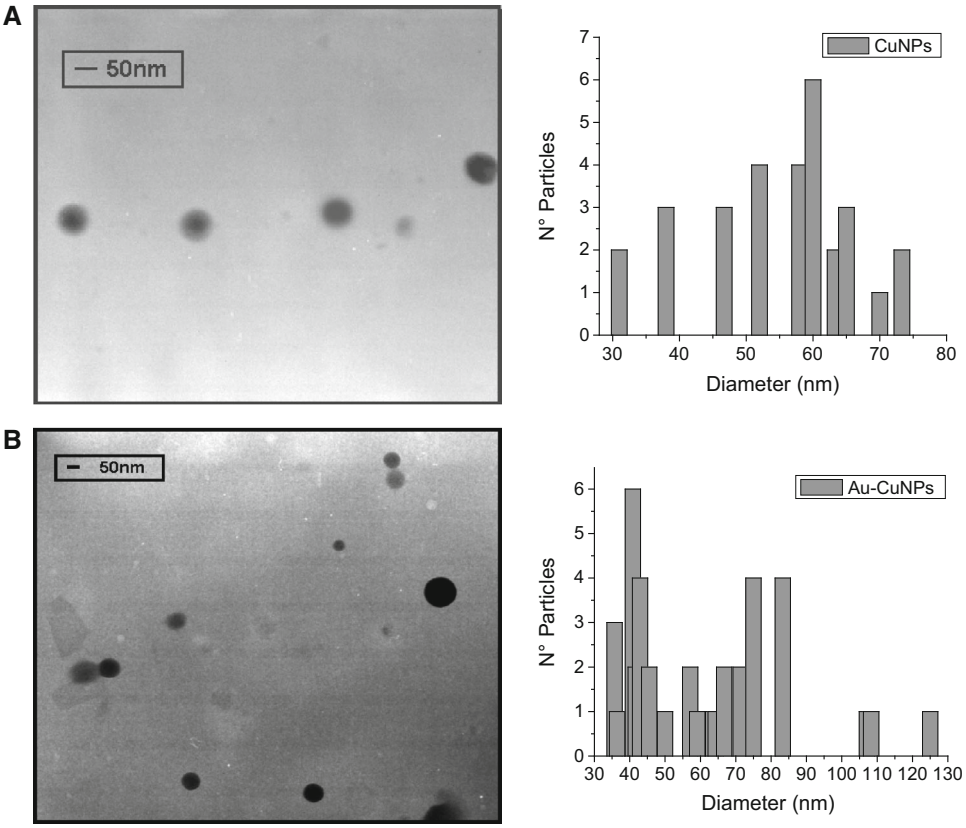

Fig. 4 TEM Micrographs and histogram of **a** CuNPs and **b** Au–CuNPs supported on α-CD/DA IC

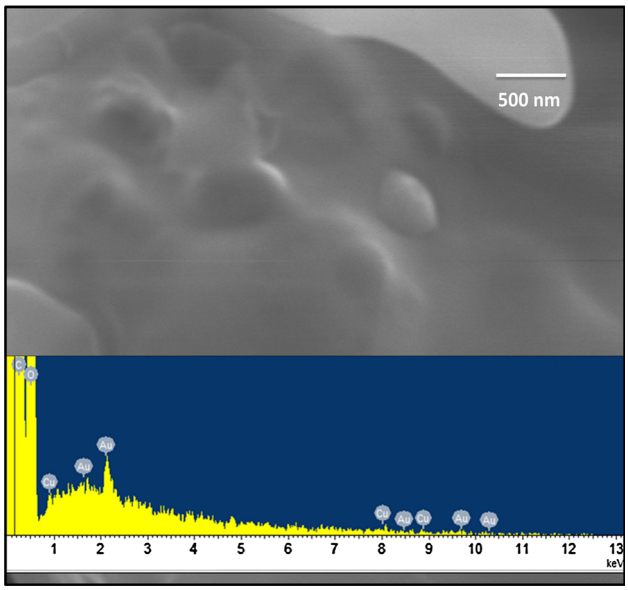

Fig. 5 SEM micrograph and EDS analysis of Au–CuNPs supported on α-CD/DA IC crystals

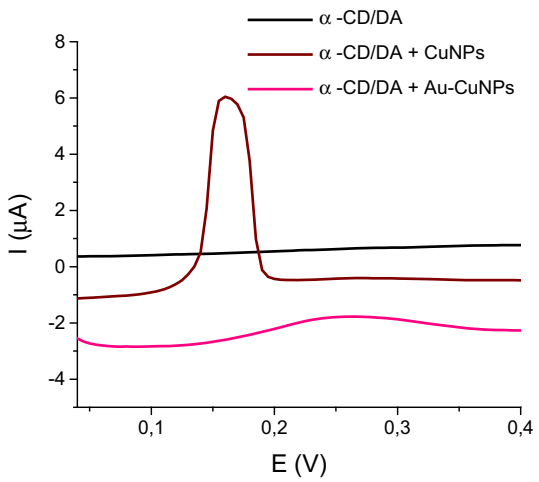

Fig. 6 Voltammograms of IC, CuNPs and Au–CuNPs supported on IC

disappeared because of the coating of the CuNPs by Au, confirming the production of core–shell NPs.

X-ray photoelectron spectroscopy (XPS) was been used in the last years, for the study of core–shell structure type [37–39]. The Fig. 7 (top) shows the high-resolution XPS spectra with a scanning range from 925 to 945 eV for the IC conjugated to Au–CuNPs. A peak at 932.73 eV was observed, which corresponds to the characteristic Cu 2*p* 3/2 electron binding energy (BE) of Cu(0). The absence of peaks at higher binding energies indicates that Cu_2O and CuO species are not present [40, 41].

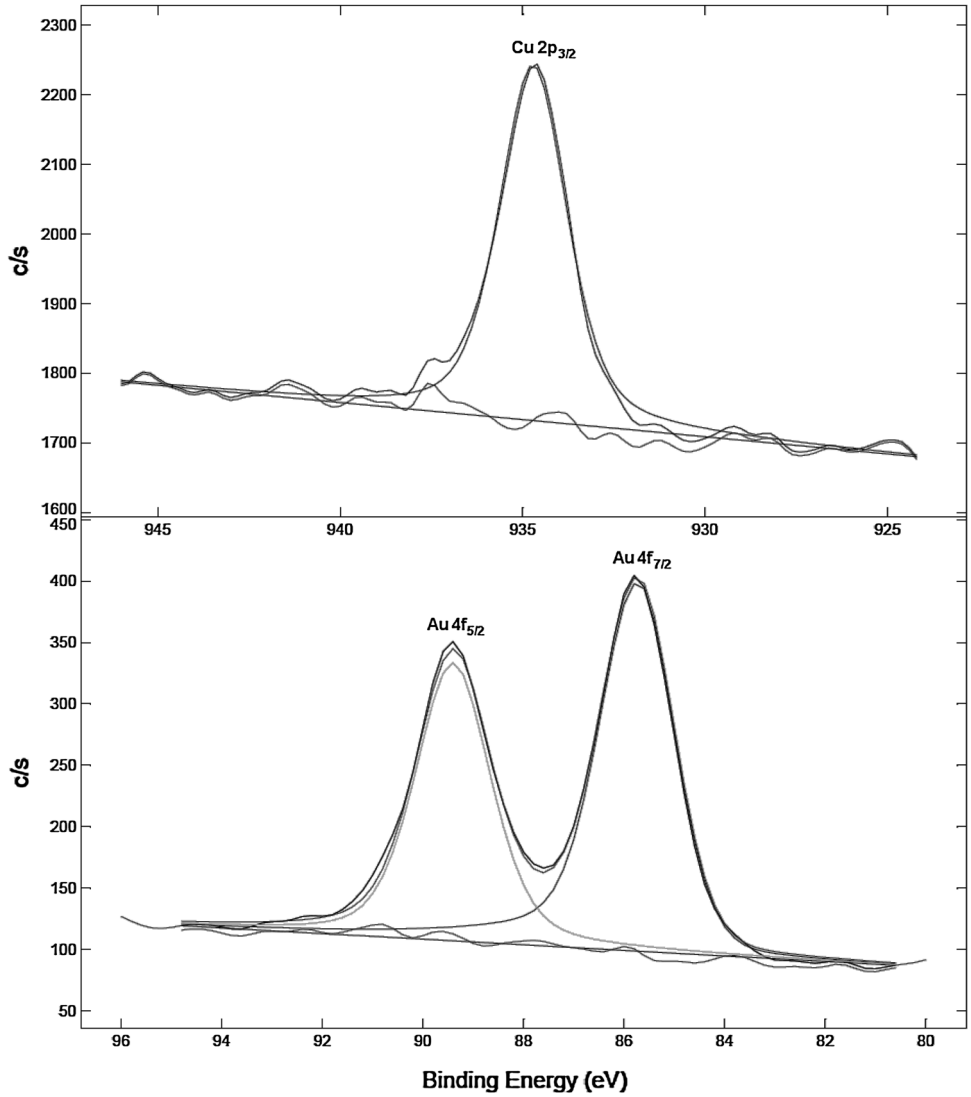

Fig. 7 High-resolution XPS spectra corresponding to binding energies of the Cu 2p (*top*) and Au 4f electrons (*bottom*) of α-CD/DA IC conjugated to Au–CuNPs. The original spectrum with fitting curves is observed

Alternatively, Fig. 7 (bottom) shows the high-resolution XPS spectra with a scanning range from 80 to 96 eV, in which a double peak appears at 83.74 and 87.41 eV, corresponding to Au 4*f* 7/2 and Au 4*f* 5/2 electron BE, respectively, characteristic of Au(0) [42]. These results confirm the coating of the copper NPs with gold. The formation of core–shell Cu–Au by sputtering is thus an effective method to prevent the oxidation of Cu particles with potential application in nanoelectronics.

Conclusion

The preparation and characterization of a new α-CD IC was achieved. ^{1}H-NMR and 2D-ROESY experiments confirmed the inclusion process and allowed the determination of the geometry of the new supramolecular structures. Additionally in this work, we demonstrated that α-CD-DA IC crystals are adequate substrates for the production of spherical copper NPs and the formation of Cu–Au core–shell metallic structures by the sputtering process. TEM and UV–Vis spectrophotometry confirmed the formation of the NPs. SEM–EDS provides additional evidence of the composition core–shell structure with rate atomic 15Cu:11Au. The anodic stripping voltammetry provides unequivocal evidence of gold coating copper particles by sputtering process. The voltamogramms show that the oxidation potential of Cu disappears when the Cu–Au core–shell is formed.

The presence of metallic copper and the absence of copper oxides were determined by XPS. This analysis confirms the gold coating of the copper particles, avoiding contact with the air and preventing oxidation. These results show that the formation of core–shell Cu–Au by sputtering

is an effective way to prevent the oxidation of Cu particles, leading to potential applications in nanoelectronics.

Experimental

General methods

All chemical reagents were commercially available and used as received. DA (Sigma-Aldrich), α-CD, (Sigma-Aldrich), and water for chromatography (Merck).

All ^{1}H-NMR spectra were recorded at 400 MHz in a Bruker Advance 400 MHz superconducting ^{1}H-NMR spectrometer in dimethyl sulfoxide-d_6 (DMSO-d_6). The ^{1}H-NMR spectra were obtained at 300 K.

For the 2D-ROESY ^{1}H-NMR method, the wg-ROESY (Watergate-ROESY) pulse sequence was used. 2D-ROESY measurements were performed using the following experimental conditions: 64 scans, 0.150 s acquisition time, 8 s pulse delay and 1024 data points.

PXRD data were collected at room temperature on a Siemens-Bruker model D 5000 powder diffractometer with Cu (K$\alpha = 1.54098$ Å) in the range of $2° < 2\theta < 30°$ (operating at 40 kV and 40 mA with a step of 0.05°/s). The lattice parameters and refinement were calculated by the SHELXS-97 method.

A Shimadzu UV-3101PC spectrophotometer was used for the absorbance measurements. Spectra were recorded between 500 and 600 nm. The results of diffuse reflectance were transformed to absorbance units by means of Kubelka–Munk conversion.

TEM micrographics was performed using a JEOL 2000FX Electron Microscope (50 kV). SEM micrographics and EDS analysis was performed using a SEM LEO 1420VP (15.00 kV).

XPS spectra were recorded on a Perkin Elmer model 1257 photoelectron spectrometer fitted with an ultra-high vacuum main chamber, a hemispherical electron analyser and an X-ray source providing unfiltered Al Kα radiation. Energy calibration was completed by assigning a BE of 284.8 eV to the C 1 s peak.

Inclusion compound (IC) preparation

The IC crystals were prepared followed protocols previously described for other ICs [9]. The ICs were obtained from 310 μL of DA with a saturated solution of 1.00 g α-CD in approximately 10 mL of water. The liquid guest was added with constant stirring and the formation of white powder was indicative of the IC formation. After 48 h, the IC crystals were filtered and washed with water and methanol to remove excess α-CD and DA, respectively. The IC crystals were then dried under vacuum for 4 h. Yields: α-CD/OA, 82.4 %.

Obtaining metal nanoparticles

A K575XD Turbo Sputter Coater was used for the formation of NPs. Copper and gold target cathodes were utilized in the sputtering equipment. The IC powder on the slides was placed on the sputtering camera with 1 mbar vacuum and Ar flow throughout. The Ar was ionized with an electric current of 15 mA. The CuNPs were formed from atoms present in the plasma onto the IC crystals. Subsequently, gold atoms were deposited onto the copper NPs in the sputtering process [14].

References

1. Wang, Y., Wong, J.F., Teng, X.W., Lin, X.Z., Yang, H.: "Pulling" nanoparticles into water: phase transfer of oleic acid stabilized monodisperse nanoparticles into aqueous solutions of α-cyclodextrin. Nano Lett. **3**, 1555 (2003)
2. Lala, N., Lalbegi, S., Adyanthaya, S., Sastry, M.: Phase transfer of aqueous gold colloidal particles capped with inclusion complexes of cyclodextrin and alkanethiol molecules into chloroform. Langmuir **17**, 3766–3768 (2001)
3. Liu, Y., Male, K.B., Bouvrette, P., Luong, J.H.T.: Control of the size and distribution of gold nanoparticles by unmodified cyclodextrins. Chem. Mater. **15**, 4172–4180 (2003)
4. Liu, J., Ong, W., Roman, E., Lynn, M., Kaifer, A.: Cyclodextrin-modified gold nanospheres. Langmuir **16**, 3000–3002 (2000)
5. Kabashin, A.V., Meunier, M., Kingston, C., Luong, J.H.T.: Fabrication and characterization of gold nanoparticles by femtosecond laser ablation in an aqueous solution of cyclodextrins. J. Phys. Chem. B **107**, 4527–4531 (2003)
6. Herrera, B., Adura, C., Yutronic, N., Kogan, M., Jara, P.: Selective nanodecoration of modified cyclodextrin crystals with gold nanorods. J. Colloid Interface Sci. **389**, 42–45 (2013)
7. Barrientos, L., Allende, P., Orellana, C., Jara, P.: Ordered arrangements of metal nanoparticles on alpha-cyclodextrin inclusión complexes by magnetrón sputtering. Inorg. Chim. Acta **380**, 372–377 (2012)
8. Rodriguez-Llamazares, S., Jara, P., Yutronic, N., Noyong, M., Bretschneider, J., Simon, U.: Face preferred deposition of gold nanoparticles α-cyclodextrin/octanethiol inclusion compound. J. Colloid Interface Sci. **316**, 202–205 (2007)
9. Rodríquez-Llamazares, S., Yutronic, N., Jara, P., Noyong, M., Bretschneider, J., Simon, U.: The structure of the first supramolecular α-cyclodextrin complex with an aliphatic monofunctional carboxylic acid. Eur. J. Org. Chem. **26**, 4298–4300 (2007)
10. Jara, P., Barrientos, L., Herrera, B., Sobrados, I.: Inclusion compounds of α-cyclodextrin with alkylthiols. J. Chil. Chem. Soc. **53**, 1474–1476 (2008)
11. Díaz, M., Silva, N., Yutronic, N., Peña, E., Chornik, B., Jara, P.: γ-Cyclodextrin/alkylthiol inclusion compounds crystals as substrates for the formation and immobilization of gold nanoparticles produced by magnetron sputtering. Incl. Phenom. Macrocycl, Chem (2014)
12. Rodríguez-Llamazares, S., Jara, P., Yutronic, N., Noyong, N., Simon, U.: Preferential adhesion of silver nanoparticles onto

crystal faces of α-cyclodextrin/carboxylic acids inclusion compounds. J. Nanosci. Nanotechnol. **12**, 8929–8934 (2012)
13. Jara, P., Justiniani, M., Yutronic, N., Sobrados, I.: Syntheses and structural aspects of cyclodextrin/dialkylamine inclusion compounds. J Incl. Phenom. **32**, 1–8 (1998)
14. Silva, N., Moris, S., Herrera, B., Diaz, M., Kogan, M., Barrientos, L., Yutronic, N., Jara, P.: Formation of copper nanoparticles supported onto inclusion compounds of α-cyclodextrin: a new route to obtain copper nanoparticles. Mol. Cryst. Liq. Cryst. **521**, 246–252 (2010)
15. Huang, H.H., Yan, F.Q., Kek, Y.M., Chew, C.H., Xu, G.Q., Ji, W., Oh, P.S., Tang, S.H.: Synthesis, characterization, and nonlinear optical properties of copper nanoparticles. Langmuir **13**, 172–175 (1997)
16. Dhas, N.A., Raj, C.P., Gedanken, A.: Synthesis, characterization, and properties of metallic copper nanoparticles. Chem. Mater. **10**, 1446–1452 (1998)
17. Zongwen, L., Yoshio, B.: A novel method for preparing copper nanorods and nanowires. Adv. Mater. **15**, 303–305 (2003)
18. Zhua, H.T., Zhang, C.Y., Yin, Y.S.: Rapid synthesis of copper nanoparticles by sodium hypophosphite reduction in ethylene glycol under microwave irradiation. J. Cryst. Growth **270**, 722–728 (2004)
19. Qi, L.M., Ma, J.M., Shen, J.L.: Synthesis of copper nanoparticles in nonionic water-in-oil microemulsions. J. Colloid Interface Sci. **186**, 498–500 (1997)
20. Lisiecki, I., Biorling, M., Motte, L., Ninham, B., Pileni, M.P.: Synthesis of copper nanosize particles in anionic reverse micelles: effect of the addition of a cationic surfactant on the size of the crystallites. Langmuir **11**, 2385–2392 (1995)
21. Cioffi, N., Torsi, L., Ditaranto, N., Tantillo, G., Ghibelli, L., Sabbatini, L., Bleve-Zacheo, T., D'Alessio, M., Zambonin, P.G., Traversa, E.: Copper nanoparticle/polymer composites with antifungal and bacteriostatic properties. Chem. Mater. **17**, 5255–5262 (2005)
22. Ren, G., Hu, D., Cheng, E.W.C., Vargas-Reus, M.A., Reip, P., Allaker, R.P.: Characterisation of copper oxide nanoparticles for antimicrobial applications. Int. J. Antimicrob. Agent **33**, 587–590 (2009)
23. Ramyadevi, J., Jeyasubramanian, K., Marikani, A., Rajakumar, G., Rahuman, A.A.: Synthesis and antimicrobial activity of copper nanoparticles. Mater. Lett. **71**, 114–116 (2012)
24. Wang, H., Huang, Y., Tan, Z., Hu, X.: Fabrication and characterization of copper nanoparticle thin-films and the electrocatalytic behavior. Anal. Chim. Acta **526**(526), 13–17 (2004)
25. Harne, S., Sharma, A., Dhaygude, M., Joglekar, S., Kodam, K., Hudlikar, M.: Novel route for rapid biosynthesis of copper nanoparticles using aqueous extract of *Calotropis procera* L. latex and their cytotoxicity on tumor cells. Colloid Surface B. **95**, 284–288 (2012)
26. Lee, Y., Choi, J., Lee, K., Stott, N., Kim, D.: Large-scale synthesis of copper nanoparticles by chemically controlled reduction for applications of inkjet-printed electronics. Nanotechnology **19**, 415604-1–415604-7 (2008)
27. Kim, J.H., Ehrman, S.H., Germer, T.A.: Influence of particle oxide coating on light scattering by submicron metal particles on silicon wafers. Appl. Phys. Lett. **84**, 1278–1280 (2004)
28. Yeshchenko, O.A., Dmytruk, I.M., Alexeenko, A.A., Dmytruk, A.M.: Size-dependent melting of spherical copper nanoparticles embedded in a silica matrix. Phys. Rev. B. **75**, 085434-1–085434-6 (2007)
29. Zong, R.L., Zhou, J., Li, B., Fu, M., Shi, S.K., Li, L.T.: Optical properties of transparent copper nanorod and nanowire arrays embedded in anodic alumina oxide. J. Chem. Phys. **123**, 094710-1–094710-5 (2005)
30. Wang, Y., Asefa, T.: Poly(allylamine)-stabilized colloidal copper nanoparticles: synthesis, morphology, and their surface-enhanced Raman scattering properties. Langmuir **26**, 7469–7474 (2010)
31. Barrientos, L., Lang, E., Zapata-Torres, G., Celis-Barros, C., Orellana, C., Jara, P., Yutronic, N.: Structural elucidation of supramolecular alpha-cyclodextrin dimer/aliphatic monofunctional molecules complexes. J. Mol. Model. **19**, 2119–2126 (2013)
32. Caira, M.R.: On the isostructurality of cyclodextrin inclusion complexes and its practical utility. Rev. Roum. Chim. **46**, 371–386 (2001)
33. Creighton, J.A., Eadon, D.G.: Ultraviolet–visible absorption spectra of the colloidal metallic elements. J. Chem. Soc. **87**, 3881–3891 (1991)
34. Pestryakov, A.N., Petranovskii, V.P., Kryazhov, A., Ozhereliev, O., Pfänder, N., Knop-Gericke, A.: study of copper nanoparticles formation on supports of different nature by UV-Vis diffuse reflectance spectroscopy. Chem. Phys. Lett. **385**, 173–176 (2004)
35. Barrientos, L., Yutronic, N., del Monte, F., Gutierrez, M.C., Jara, P.: Ordered arrangement of gold nanoparticles an α-cyclodextrin-dodecanethiol inclusion compound produced by magneton sputtering. New J. Chem. **31**, 1400–1402 (2007)
36. Van Staden, J.F., Matoetoe, M.C.: Simultaneous determination of copper, lead, cadmium and zinc using differential pulse anodic stripping voltammetry in a flow system. Anal. Chim. Acta **411**, 201–207 (2000)
37. Cao, W., Li, W., Yin, R., Zhou, W.: Controlled fabrication of Cu–Sn core–shell nanoparticles via displacement reaction. Colloid Surf. A **453**, 37–43 (2014)
38. Penga, Y., Yang, C., Chene, K., Popuri, S.R., Lee, C.H., Tang, B.S.: Study on synthesis of ultrafine Cu–Ag core–shell powders with high electrical conductivity. Appl. Surf. Sci. **263**, 38–44 (2012)
39. Zhao, J., Zhang, D., Zhao, J.: Fabrication of Cu–Ag core–shell bimetallic superfine powders by eco-friendly reagents and structures characterization. J. Solid State Chem. **184**, 2339–2344 (2011)
40. Hoppe, R., Miiller, H.P., Politis, C., Steiner, P., Kinsinger, V., Sander, I., Siegwart, B., Hiifner, S.Z.: The Cu valence in the high Tc superconductors and in monovalent, divalent and trivalent copper oxides determined from XPS core level spectroscopy. Z. Phys. B Condens. Matter **67**, 497–502 (1987)
41. Espinós, J.P., Morales, J., Barranco, A., Caballero, A., Holgado, J.P., González-Elipe, A.R.: Interface effects for Cu, CuO, and Cu_2O deposited on SiO_2 and ZrO_2 XPS. Determination of the valence state of copper in Cu/SiO_2 and Cu/ZrO_2 catalysts. J. Phys. Chem. B **106**, 6921–6929 (2002)
42. Joseph, Y., Besnard, I., Rosenberger, M., Guse, B., Nothofer, H.G., Wessels, J.M., Wild, U., Knop-Gericke, A., Su, D., Schlögl, R., Yasuda, A., Vossmeyer, T.: Self-assembled gold nanoparticle/alkanedithiol films: preparation, electron microscopy, xps-analysis, charge transport, and vapor-sensing properties. J. Phys. Chem. B **107**, 7406–7413 (2003)